RESEARCH ARTICLE SUMMARY

COSMOCHEMISTRY

Samples returned from the asteroid Ryugu are similar to Ivuna-type carbonaceous meteorites

Tetsuya Yokoyama† and Kazuhide Nagashima† *et al.*

INTRODUCTION: The Hayabusa2 spacecraft made two landings on the asteroid (162173) Ryugu in 2019, during which it collected samples of the surface material. Those samples were delivered to Earth in December 2020. The colors, shapes, and morphologies of the returned samples are consistent with those observed on Ryugu by Hayabusa2, indicating that they are representative of the asteroid. Laboratory analysis of the samples can determine the chemical composition of Ryugu and provide information on its formation and history.

RATIONALE: We used laboratory analysis to inform the following questions: (i) What are the elemental abundances of Ryugu? (ii) What are the isotopic compositions of Ryugu? (iii) Does Ryugu consist of primary materials produced in the disk from which the Solar System formed or of secondary materials produced in the asteroid or on a parent asteroid? (iv) When were Ryugu's constituent materials formed? (v) What, if any, relationship does Ryugu have with meteorites?

RESULTS: We quantified the abundances of 66 elements in the Ryugu samples: H, Li, Be, C, O, Na, Mg, Al, Si, P, S, Cl, K, Ca, Sc, Ti, V, Cr, Mn, Fe, Co, Ni, Cu, Zn, Ga, Ge, As, Se, Rb, Sr, Y, Zr, Nb, Mo, Ru, Rh, Pd, Ag, Cd, In, Sn, Te, Cs, Ba, La, Ce, Pr, Nd, Sm, Eu, Gd, Tb, Dy, Ho, Er, Tm, Yb, Lu, Hf, Ta, W, Tl, Pb, Bi, Th, and U. There is a slight variation in chemical compositions between samples from the first and second touchdown sites, but the variations could be due to heterogeneity among the samples that were analyzed.

The Cr-Ti isotopes and abundance of volatile elements are similar to those of carbonaceous meteorites in the CI (Ivuna-like) chondrite group. The Ryugu samples consist of the minerals magnetite, breunnerite, dolomite, and pyrrhotite as grains embedded in a matrix composed of serpentine and saponite. This mineral assemblage and the texture are also similar to those of CI meteorites. Anhydrous silicates are almost absent, which indicates extensive liquid water–rock reactions (aqueous alteration) in the material. We conclude that the samples mainly consist of secondary materials that were formed by aqueous alteration in a parent body, from which Ryugu later formed.

The oxygen isotopes in the bulk Ryugu samples are also similar to those in CI chondrites. We used oxygen isotope thermometry to determine the temperature at which the dolomite and magnetite precipitated from an aqueous solution, which we found to be 37° ± 10°C. The ^{53}Mn-^{53}Cr isotopes date the aqueous alteration at $5.2^{+0.8}_{-0.7}$ million (statistical) or $5.2^{+1.6}_{-2.1}$ million (systematic) years after the birth of the Solar System.

Phyllosilicate minerals are the main host of water in the Ryugu samples. The amount of structural water in Ryugu is similar to that in CI chondrites, but interlayer water is largely absent in Ryugu, which suggests a loss of interlayer water to space. The abundance of structural water and results from dehydration experiments indicate that the Ryugu samples remained below ~100°C from the time of aqueous alteration until the present. We ascribe the removal of interlayer water to a combination of impact heating, solar heating, solar wind irradiation, and long-term exposure to the ultrahigh vacuum of space. The loss of interlayer water from phyllosilicates could be responsible for the comet-like activity of some carbonaceous asteroids and the ejection of solid material from the surface of asteroid Bennu.

CONCLUSION: The Ryugu samples are most similar to CI chondrite meteorites but are more chemically pristine. The chemical composition of the Ryugu samples is a closer match to the Sun's photosphere than to the composition of any other natural samples studied in laboratories. CI chondrites appear to have been modified on Earth or during atmospheric entry. Such modification of CI chondrites could have included the alteration of the structures of organics and phyllosilicates, the adsorption of terrestrial water, and the formation of sulfates and ferrihydrites. Those issues do not affect the Ryugu samples. Those modifications might have changed the albedo, porosity, and density of the CI chondrites, causing the observed differences between CI meteorites, Hayabusa2 measurements of Ryugu's surface, and the Ryugu samples returned to Earth. ■

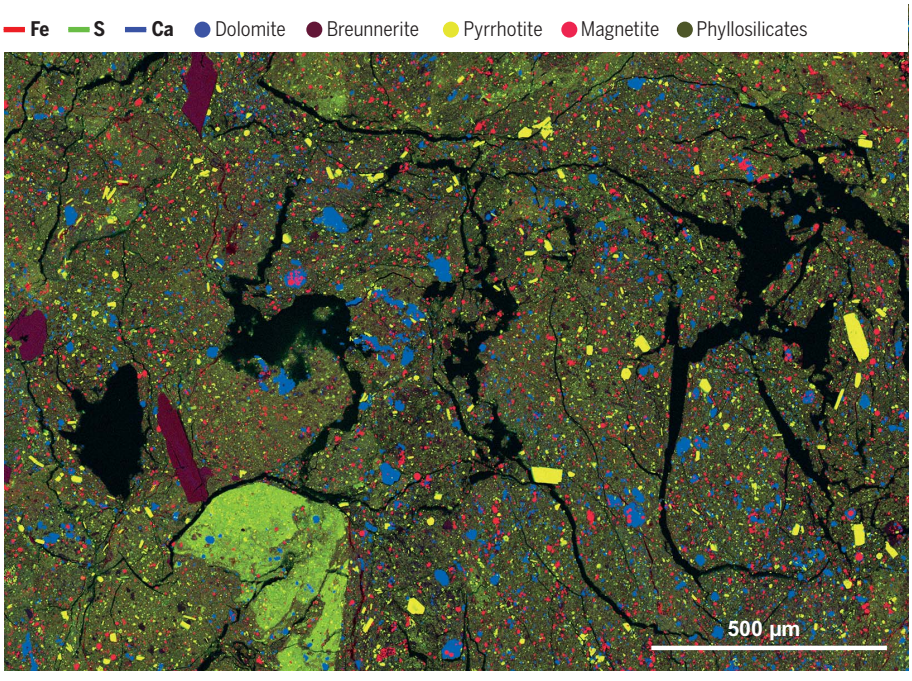

Representative petrography of a Ryugu sample, designated C0002-C1001. Colors indicate elemental abundances determined from x-ray spectroscopy. Lines of iron, sulfur, and calcium are shown as red, green, and blue (RGB) color channels in that order. Combinations of these elements are assigned to specific minerals, as indicated in the legend. All visible minerals were formed by aqueous alteration on Ryugu's parent body.

The complete list of authors and their affiliations is available in the full article online.
***Corresponding author: Hisayoshi Yurimoto (yuri@ep.sci.hokudai.ac.jp)**
†These authors contributed equally to this work.
Cite this article as T. Yokoyama *et al.*, *Science* 379, eabn7850 (2023). DOI: 10.1126/science.abn7850

RESEARCH ARTICLE

COSMOCHEMISTRY

Samples returned from the asteroid Ryugu are similar to Ivuna-type carbonaceous meteorites

Tetsuya Yokoyama[1]†, Kazuhide Nagashima[2]†, Izumi Nakai[3], Edward D. Young[4], Yoshinari Abe[5], Jérôme Aléon[6], Conel M. O'D. Alexander[7], Sachiko Amari[8], Yuri Amelin[9], Ken-ichi Bajo[10], Martin Bizzarro[11], Audrey Bouvier[12], Richard W. Carlson[7], Marc Chaussidon[13], Byeon-Gak Choi[14], Nicolas Dauphas[15], Andrew M. Davis[15], Tommaso Di Rocco[16], Wataru Fujiya[17], Ryota Fukai[18], Ikshu Gautam[1], Makiko K. Haba[1], Yuki Hibiya[19], Hiroshi Hidaka[20], Hisashi Homma[21], Peter Hoppe[22], Gary R. Huss[2], Kiyohiro Ichida[23], Tsuyoshi Iizuka[24], Trevor R. Ireland[25], Akira Ishikawa[1], Motoo Ito[26], Shoichi Itoh[27], Noriyuki Kawasaki[10], Noriko T. Kita[28], Kouki Kitajima[28], Thorsten Kleine[29], Shintaro Komatani[23], Alexander N. Krot[2], Ming-Chang Liu[4], Yuki Masuda[1], Kevin D. McKeegan[4], Mayu Morita[23], Kazuko Motomura[30], Frédéric Moynier[13], Ann Nguyen[31], Larry Nittler[7], Morihiko Onose[23], Andreas Pack[16], Changkun Park[32], Laurette Piani[33], Liping Qin[34], Sara S. Russell[35], Naoya Sakamoto[36], Maria Schönbächler[37], Lauren Tafla[4], Haolan Tang[4], Kentaro Terada[38], Yasuko Terada[39], Tomohiro Usui[18], Sohei Wada[10], Meenakshi Wadhwa[40], Richard J. Walker[41], Katsuyuki Yamashita[42], Qing-Zhu Yin[43], Shigekazu Yoneda[44], Hiroharu Yui[45], Ai-Cheng Zhang[46], Harold C. ConnollyJr.[47], Dante S. Lauretta[48], Tomoki Nakamura[49], Hiroshi Naraoka[50], Takaaki Noguchi[27], Ryuji Okazaki[50], Kanako Sakamoto[18], Hikaru Yabuta[51], Masanao Abe[18], Masahiko Arakawa[52], Atsushi Fujii[18], Masahiko Hayakawa[18], Naoyuki Hirata[52], Naru Hirata[53], Rie Honda[54], Chikatoshi Honda[53], Satoshi Hosoda[18], Yu-ichi Iijima[18]‡, Hitoshi Ikeda[18], Masateru Ishiguro[14], Yoshiaki Ishihara[18], Takahiro Iwata[18,55], Kosuke Kawahara[18], Shota Kikuchi[56], Kohei Kitazato[53], Koji Matsumoto[57], Moe Matsuoka[18]§, Tatsuhiro Michikami[58], Yuya Mimasu[18], Akira Miura[18], Tomokatsu Morota[24], Satoru Nakazawa[18], Noriyuki Namiki[57], Hirotomo Noda[57], Rina Noguchi[59], Naoko Ogawa[18], Kazunori Ogawa[18], Tatsuaki Okada[18,60], Chisato Okamoto[52]‡, Go Ono[18], Masanobu Ozaki[18,55], Takanao Saiki[18], Naoya Sakatani[61], Hirotaka Sawada[18], Hiroki Senshu[56], Yuri Shimaki[18], Kei Shirai[18], Seiji Sugita[24], Yuto Takei[18], Hiroshi Takeuchi[18], Satoshi Tanaka[18], Eri Tatsumi[62], Fuyuto Terui[63], Yuichi Tsuda[18], Ryudo Tsukizaki[18], Koji Wada[56], Sei-ichiro Watanabe[20], Manabu Yamada[56], Tetsuya Yamada[18], Yukio Yamamoto[18], Hajime Yano[18], Yasuhiro Yokota[18], Keisuke Yoshihara[18], Makoto Yoshikawa[18], Kent Yoshikawa[18], Shizuho Furuya[18], Kentaro Hatakeda[64], Tasuku Hayashi[18], Yuya Hitomi[64], Kazuya Kumagai[64], Akiko Miyazaki[18], Aiko Nakato[18], Masahiro Nishimura[18], Hiromichi Soejima[64], Ayako Suzuki[64], Toru Yada[18], Daiki Yamamoto[18], Kasumi Yogata[18], Miwa Yoshitake[18], Shogo Tachibana[65], Hisayoshi Yurimoto[10,36]*

Carbonaceous meteorites are thought to be fragments of C-type (carbonaceous) asteroids. Samples of the C-type asteroid (162173) Ryugu were retrieved by the Hayabusa2 spacecraft. We measured the mineralogy and bulk chemical and isotopic compositions of Ryugu samples. The samples are mainly composed of materials similar to those of carbonaceous chondrite meteorites, particularly the CI (Ivuna-type) group. The samples consist predominantly of minerals formed in aqueous fluid on a parent planetesimal. The primary minerals were altered by fluids at a temperature of 37° ± 10°C, about $5.2^{+0.8}_{-0.7}$ million (statistical) or $5.2^{+1.6}_{-2.1}$ million (systematic) years after the formation of the first solids in the Solar System. After aqueous alteration, the Ryugu samples were likely never heated above ~100°C. The samples have a chemical composition that more closely resembles that of the Sun's photosphere than other natural samples do.

Meteorites are fragments of asteroids, but identifications of the specific parent asteroid are rarely available. Samples of asteroid (25143) Itokawa that were returned by the Hayabusa mission showed that S-type (stony, in a remote sensing classification) asteroids are composed of materials that are consistent with those of ordinary chondrite meteorites (*1*, *2*). The Hayabusa2 (*3*) spacecraft was launched on 2014 December 3 to collect samples of the near-Earth asteroid (162173) Ryugu, which is Cb-type [a subclass of C-type (carbonaceous) asteroid in the remote sensing classification]. A mission goal was to determine the relationship between C-type asteroids and the carbonaceous chondrite meteorites. Observations of Ryugu from Hayabusa2 after rendezvous showed that (i) Ryugu is darker than every meteorite group (*4*, *5*), (ii) Ryugu contains ubiquitous phyllosilicate minerals (*4*, *6*), (iii) Ryugu's surface experienced heating above 300°C (*6*), and (iv) Ryugu materials are probably more porous than carbonaceous chondrites (*7*, *8*). These results indicated that carbonaceous chondrites are plausible analogs of Ryugu but do not completely match the spacecraft observations. Laboratory analysis of the samples of Ryugu returned by Hayabusa2 is required to explain these results.

During 2019, the Hayabusa2 spacecraft made two landings on Ryugu to collect materials (*9*); it then delivered the collected samples to Earth on 2020 December 6. The returned samples are rock fragments that range in size up to ~10 mm in length, with a total mass of 5.4 g. Their colors, shapes, and morphologies are consistent with those observed on the surface by Hayabusa2, indicating that the returned samples are representative of Ryugu's surface (*10*, *11*). The samples were recovered in a nondestructive manner and examined under contamination-controlled conditions at the Japan Aerospace Exploration Agency (JAXA) Extraterrestrial Sample Curation Center before delivery to initial analysis teams in June 2021 (*10*). Our team was allocated ~125 mg of samples, which contained both powder and particles from the first and the second touchdown sites (*12*). We used ~95 mg for this paper.

Petrology and mineralogy

We prepared polished sections of particle samples that were retrieved from the first touchdown site (particle designation A0058) and from the second touchdown site (C0002) (*12*). The petrography, mineralogy, and chemical composition of the minerals were determined using electron microscopy (*12*).

The Ryugu samples are mixtures of mechanical fragments—composed of fine-grained materials of phyllosilicate minerals, predominantly serpentine and saponite—and coarser grains dominated by carbonates, magnetite, and sulfides (Fig. 1, A, B, and D). No Ca-Al–rich inclusions (CAIs) or chondrules, which are characteristic constituents of most chondrite meteorites, were evident in the allocated samples. The serpentine-to-saponite molar ratio is about 3:2 on the basis of the chemical compositions of the phyllosilicate minerals (Fig. 1C). The coarser-grained minerals in the polished sections are dolomite [$CaMg(CO_3)_2$], breunnerite [$(Mg, Fe, Mn)CO_3$], pyrrhotite ($Fe_{1-x}S$, where x = 0 to 0.17), and magnetite (Fe_3O_4) (Fig. 1B). These are distributed throughout the sections (Fig. 1D) and in small veins (Fig. 1A). Calcite ($CaCO_3$), pentlandite [$(Fe,Ni)_9S_8$], cubanite ($CuFe_2S_3$), ilmenite ($FeTiO_3$), apatite [$(Ca_5(PO_4)_3(OH,F,Cl)$], and Mg-Na-phosphate are present as accessory minerals. Anhydrous silicates, such as olivine and pyroxene, are common in chondrites but are very rare in our Ryugu samples, occurring only as discrete grains smaller than ~10 μm across. No metal grains were identified. Overall, the petrology and mineralogy of the Ryugu samples most closely resemble those of the CI (Ivuna-like) group of chondrite

meteorites, which have experienced extensive aqueous alteration (*13*). However, sulfates and ferrihydrite, which are commonly observed in CI chondrites, were not identified in the Ryugu samples that we studied.

Bulk chemical and isotopic compositions

Bulk chemical compositions were determined using ~25 mg of small-grain aggregate samples from each site: particles A0106 and A0107 from the first touchdown site and C0108 from the second touchdown site (*12*). Elemental abundances were determined using x-ray fluorescence (XRF) analysis and inductively coupled plasma mass spectrometry (ICP-MS). After chemical analysis, the same samples, ICP-MS analysis, and thermal ionization mass spectrometry (TIMS) were used to determine isotopic compositions of titanium and chromium.

We found no systematic differences in chemical composition between the samples from the first and second touchdown sites (Fig. 2). We did find variations in bulk composition within each of those samples, which are most likely due to heterogeneity at small scales (*12*). The masses of the samples that were analyzed were less than 30 mg; coarser-grained water-precipitated minerals might not be uniformly distributed at that scale (a cross section of an ~10-mg block is shown in Fig. 1D). Spatial heterogeneity in the mineral distributions is observed for carbonates (dolomite) and sulfides (pyrrhotite), which both precipitate from aqueous solution and probably occurred during aqueous alteration on Ryugu's parent planetesimal (Fig. 1). We found different concentrations of rare earth elements (REEs) between samples from the first touchdown site and the second touchdown site (*12*), with both being higher than the REE abundance in CI chondrites (Fig. 2). These variable enrichments could be due to depletion of H_2O, relative to CI chondrites (see next paragraph and the section H_2O and CO_2 sources), and the heterogeneous distribution of REE-rich Ca-phosphate grains (*14*, *15*). Heterogeneity at similar scales has been observed in CI chondrites (*16*, *17*) and in the ungrouped carbonaceous chondrite Tagish Lake (*18*).

We did not observe systematic depletions of elemental abundances, relative to CI chondrites, as a function of the 50% condensation temperatures of each element (their volatility) (Fig. 2). This is unlike other groups of carbonaceous chondrites, which show various degrees of depletion with volatility (*19*). The high abundance of moderately and highly volatile elements in the Ryugu samples indicates that Ryugu is composed of materials related to the CI chondrite group. However, the elemental abundances of hydrogen and oxygen are highly depleted in the Ryugu samples compared with CI chondrites, which we interpret as being due to the removal of H_2O.

Previous studies have found a dichotomy in the isotopic compositions of titanium and chromium between noncarbonaceous (NC)–like and carbonaceous (CC)–like isotope ratios (*20*–*23*). The bulk titanium and chromium isotopic ratios we measured for the Ryugu samples are similar to the CB (Bencubbin-like) and CI chondrite values (*12*), which are both CC (Fig. 3). CB chondrites are metal rich (*24*), unlike the Ryugu samples, and so are unlikely to be directly related.

Oxygen isotopic composition

Bulk oxygen isotopic compositions of the Ryugu samples from the first (~4 mg of aggregate sample A0107) and the second (~1 mg of fragment from particle sample C0002) touchdown sites were determined using laser-fluorination isotope-ratio mass spectrometry (LF-IRMS) (*12*). Oxygen isotopic compositions of secondary minerals from the first touchdown site were determined by secondary ion mass spectrometry (SIMS) using the polished section used for petrology and mineralogy (*12*).

Oxygen isotopes measured in the bulk Ryugu samples overlap with those of the bulk samples of the Orgueil CI chondrite (Fig. 4). We interpret the variation in $\delta^{18}O$ (defined as the permille deviation from the $^{18}O/^{16}O$ ratio of standard mean ocean water) as being due to the heterogeneous distributions of the constituent minerals, which may have very different isotopic compositions, including phyllosilicates, carbonates, and magnetite. Two ~2-mg Ryugu samples from the first touchdown site have consistent $\Delta^{17}O$ values (defined as the permille deviation from

[1]Department of Earth and Planetary Sciences, Tokyo Institute of Technology, Tokyo 152-8551, Japan. [2]Hawai'i Institute of Geophysics and Planetology, University of Hawai'i at Mānoa, Honolulu, HI 96822, USA. [3]Department of Applied Chemistry, Tokyo University of Science, Tokyo 162-8601, Japan. [4]Department of Earth, Planetary, and Space Sciences, University of California, Los Angeles, CA 90095, USA. [5]Graduate School of Engineering Materials Science and Engineering, Tokyo Denki University, Tokyo 120-8551, Japan. [6]Institut de Minéralogie, de Physique des Matériaux et de Cosmochimie, Sorbonne Université, Museum National d'Histoire Naturelle, Centre National de la Recherche Scientifique Unité Mixte de Recherche 7590, Institut de recherche pour le développement, 75005 Paris, France. [7]Earth and Planets Laboratory, Carnegie Institution for Science, Washington, DC 20015, USA. [8]McDonnell Center for the Space Sciences and Physics Department, Washington University, St. Louis, MO 63130, USA. [9]Guangzhou Institute of Geochemistry, Chinese Academy of Sciences, Guangzhou, GD 510640, China. [10]Department of Natural History Sciences, Hokkaido University, Sapporo 001-0021, Japan. [11]Centre for Star and Planet Formation, Globe Institute, University of Copenhagen, K 1350 Copenhagen, Denmark. [12]Bayerisches Geoinstitut, Universität Bayreuth, 95447 Bayreuth, Germany. [13]Université de Paris, Institut de physique du globe de Paris, Centre National de la Recherche Scientifique, 75005 Paris, France. [14]Department of Physics and Astronomy, Seoul National University, Seoul 08826, Republic of Korea. [15]Department of the Geophysical Sciences and Enrico Fermi Institute, University of Chicago, Chicago, IL 60637, USA. [16]Faculty of Geosciences and Geography, University of Göttingen, D-37077 Göttingen, Germany. [17]Faculty of Science, Ibaraki University, Mito 310-8512, Japan. [18]Institute of Space and Astronautical Science/Jaxa Space Exploration Center, Japan Aerospace Exploration Agency, Sagamihara 252-5210, Japan. [19]Department of General Systems Studies, University of Tokyo, Tokyo 153-0041, Japan. [20]Department of Earth and Planetary Sciences, Nagoya University, Nagoya 464-8601, Japan. [21]Osaka Application Laboratory, Rigaku Corporation, Osaka 569-1146, Japan. [22]Max Planck Institute for Chemistry, Mainz 55128, Germany. [23]Analytical Technology Division, Horiba Techno Service Co. Ltd., Kyoto 601-8125, Japan. [24]Department of Earth and Planetary Science, University of Tokyo, Tokyo 113-0033, Japan. [25]School of Earth and Environmental Sciences, University of Queensland, St Lucia, QLD 4072, Australia. [26]Kochi Institute for Core Sample Research, Japan Agency for Marine-Earth Science and Technology, Kochi 783-8502, Japan. [27]Department of Earth and Planetary Sciences, Kyoto University, Kyoto 606-8502, Japan. [28]Department of Geoscience, University of Wisconsin, Madison, WI 53706, USA. [29]Max Planck Institute for Solar System Research, 37077 Göttingen, Germany. [30]Thermal Analysis Division, Rigaku Corporation, Tokyo 196-8666, Japan. [31]Astromaterials Research and Exploration Science Division, National Aeronautics and Space Administration Johnson Space Center, Houston, TX 77058, USA. [32]Division of Earth-System Sciences, Korea Polar Research Institute, Incheon 21990, Korea. [33]Centre de Recherches Pétrographiques et Géochimiques, Centre National de la Recherche Scientifique–Université de Lorraine, 54500 Nancy, France. [34]School of Earth and Space Sciences, University of Science and Technology of China, Anhui 230026, China. [35]Department of Earth Sciences, Natural History Museum, London SW7 5BD, UK. [36]Isotope Imaging Laboratory, Hokkaido University, Sapporo 001-0021, Japan. [37]Institute for Geochemistry and Petrology, Department of Earth Sciences, ETH Zurich, Zurich, Switzerland. [38]Department of Earth and Space Science, Osaka University, Osaka 560-0043, Japan. [39]Spectroscopy and Imaging Division, Japan Synchrotron Radiation Research Institute, Hyogo 679-5198, Japan. [40]School of Earth and Space Exploration, Arizona State University, Tempe, AZ 85281, USA. [41]Department of Geology, University of Maryland, College Park, MD 20742, USA. [42]Graduate School of Natural Science and Technology, Okayama University, Okayama 700-8530, Japan. [43]Department of Earth and Planetary Sciences, University of California, Davis, CA 95616, USA. [44]Department of Science and Engineering, National Museum of Nature and Science, Tsukuba 305-0005, Japan. [45]Department of Chemistry, Tokyo University of Science, Tokyo 162-8601, Japan. [46]School of Earth Sciences and Engineering, Nanjing University, Nanjing 210023, China. [47]Department of Geology, School of Earth and Environment, Rowan University, Glassboro, NJ 08028, USA. [48]Lunar and Planetary Laboratory, University of Arizona, Tucson, AZ 85705, USA. [49]Department of Earth Science, Tohoku University, Sendai 980-8578, Japan. [50]Department of Earth and Planetary Sciences, Kyushu University, Fukuoka 819-0395, Japan. [51]Earth and Planetary Systems Science Program, Hiroshima University, Higashi-Hiroshima 739-8526, Japan. [52]Graduate School of Science, Kobe University, Kobe 657-8501, Japan. [53]Department of Computer Science and Engineering, University of Aizu, Aizu-Wakamatsu 965-8580, Japan. [54]Faculty of Science and Technology, Kochi University, Kochi 780-8520, Japan. [55]Graduate University for Advanced Studies, Sokendai, Kanagawa 240-0193, Japan. [56]Planetary Exploration Research Center, Chiba Institute of Technology, Narashino 275-0016, Japan. [57]National Astronomical Observatory of Japan, Mitaka 181-8588, Japan. [58]Faculty of Engineering, Kinki University, Higashi-Hiroshima 739-2116, Japan. [59]Academic Assembly Institute of Science and Technology, Niigata University, Niigata 950-2181, Japan. [60]Department of Chemistry, University of Tokyo, Tokyo 113-0033, Japan. [61]College of Science Department of Physics, Rikkyo University, Tokyo 171-8501, Japan. [62]Instituto de Astrofísica de Canarias, University of La Laguna, Tenerife, Spain. [63]Graduate School of Engineering, Kanagawa Institute of Technology, Atsugi 243-0292, Japan. [64]Marine Works Japan Ltd., Yokosuka 237-0063, Japan. [65]UTokyo Organization for Planetary and Space Science, University of Tokyo, Tokyo 113-0033, Japan.

***Corresponding author. Email: yuri@ep.sci.hokudai.ac.jp** †These authors contributed equally to this work. ‡Deceased. §Present address: Laboratoire d'études spatiales et d'instrumentation en astrophysique, Observatoire de Paris, 92195 Meudon, France.

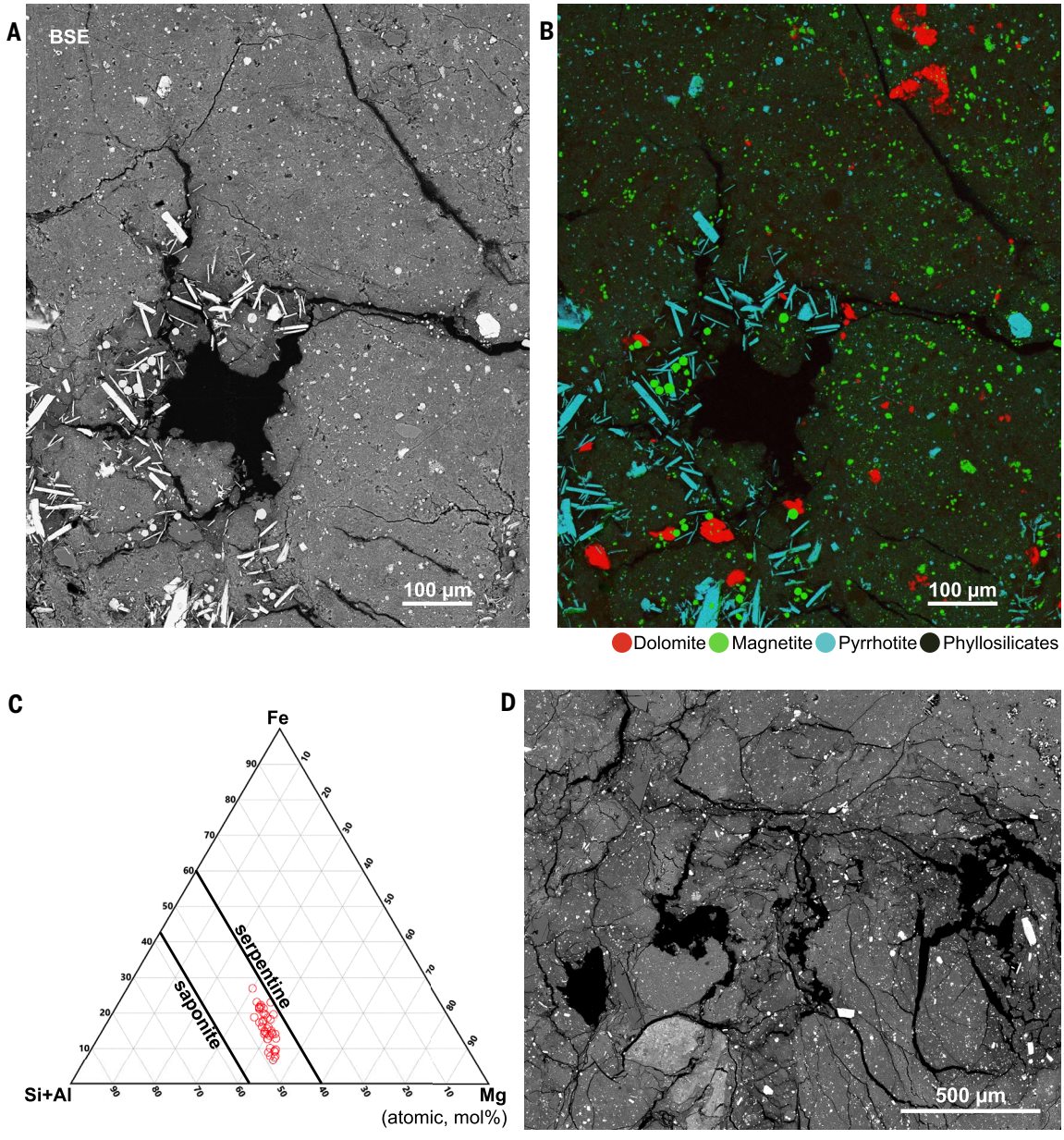

Fig. 1. Petrography of the Ryugu sample. (**A**) Backscattered electron (BSE) image of Ryugu sample A0058-C1001 (*12*). The black space in the figure is a pore. (**B**) Combined elemental map of the same sample, with characteristic x-rays of Ca Kα, Fe Kα, and S Kα lines assigned to red, green, and blue (RGB) color channels. Carbonate (dolomite), sulfide (pyrrhotite), and iron oxide (magnetite) minerals are embedded in a matrix of phyllosilicates and, in some cases, precipitated in small veins. The sulfide texture is similar to that in the ungrouped chondrite Flensburg (*52*). (**C**) Ternary diagram between Fe, Mg, and Si with Al (Si+Al) showing bulk chemical compositions of phyllosilicates in A0058-C1001. Black lines are compositions of solid solution for serpentine and saponite. Each open red circle shows the bulk chemical composition of phyllosilicates that were measured in various locations of the areas shown in (A) and (B), with each location being a 5- to 10-μm square. We chose each size to exclude minerals other than phyllosilicates in the area. The bulk compositions differ from location to location, with a distribution that indicates that the phyllosilicates consist of serpentine and saponite with variable Fe/Mg ratios. Uncertainties on each measurement are smaller than the symbol size. (**D**) BSE image of Ryugu sample C0002-C1001 showing brecciated matrix. The texture is similar to that of CI chondrites (*53*).

the terrestrial fractionation line) (*12*), with an average $\Delta^{17}O$ of 0.68 ± 0.05 per mil (‰) (uncertainty of 2 SD). These are higher $\Delta^{17}O$ values than those of the three samples of Orgueil that were analyzed in the same laboratory session, which have $\Delta^{17}O$ values of 0.42 to 0.53‰. Another Ryugu sample from the second touchdown site that was analyzed in a different laboratory has a lower $\Delta^{17}O$ value of 0.44 ± 0.05‰, which is consistent with values for Orgueil that were analyzed with the same equipment ($\Delta^{17}O$ = 0.39 to 0.57‰). We therefore ascribe the differences between the Ryugu samples as being due to heterogeneity on small scales or different sampling sites on Ryugu and not as systematic differences between the laboratories. The average $\Delta^{17}O$ value of the three Ryugu samples, 0.61 ± 0.28‰ (2 SD), is slightly higher than the average for the Orgueil samples of 0.48 ± 0.15‰ (2 SD, five samples); a single measurement of the CI chondrite Ivuna,

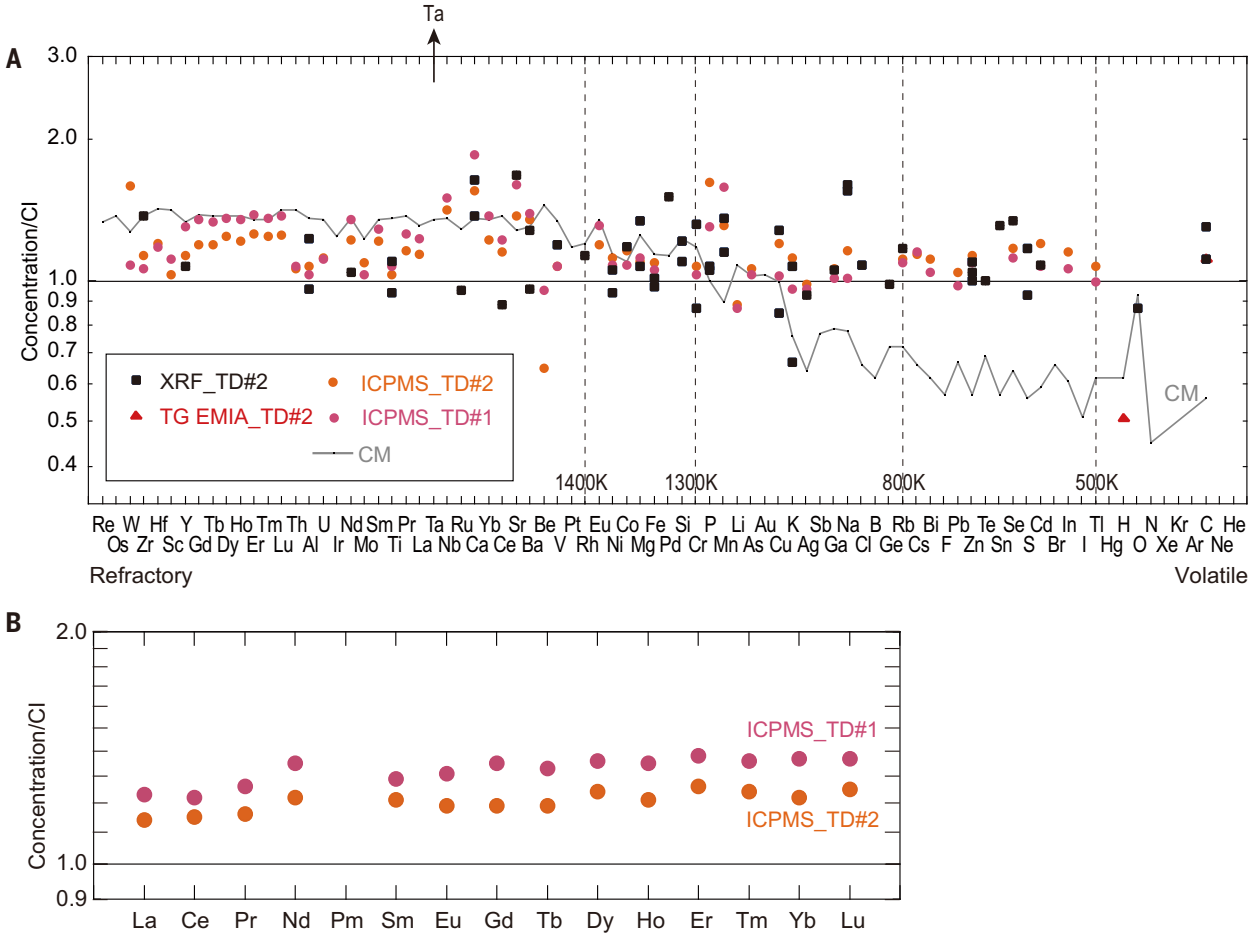

Fig. 2. Elemental abundances of Ryugu. (**A**) Measured abundances of elements in Ryugu normalized to CI chondrite values (*49*) and plotted on a logarithmic scale and as a function of 50% condensation temperature (i.e., volatility) (*49*). There is no systematic trend with condensation temperature. Black squares are results from our XRF analysis (*12*). Pink and orange circles are results from our ICP-MS analysis (*12*). Red triangles are results from our TG-MS and EMIA-Step analyses (*12*). In the legend, TD#1 and TD#2 indicate samples from the first and second touchdown sites, respectively. The high abundance of tantalum is indicated by an upward arrow, which is due to contamination by the tantalum projectiles used in the sampling process (*12*). The gray line shows representative values for CM (Mighei-type) chondrites (*49*). The horizontal black line is the 1:1 ratio. The vertical dashed lines show specific condensation temperature thresholds, as labeled. (**B**) REE abundances, plotted in order of atomic number and on a logarithmic scale. For both (A) and (B), numeric values and uncertainties are provided in data S2. Uncertainties are mostly much smaller than the variations between the samples and techniques.

which was 0.41 ± 0.05‰; and prior measurements of CI chondrites [0.39 to 0.47‰ (*25*)]. The difference may either reflect original heterogeneity between small samples or result from contamination of the meteorite samples by terrestrial water that was incorporated by the phyllosilicates, sulfates, iron oxides, and iron hydroxides. The discrepancy in the $\Delta^{17}O$ values between Ryugu and Orgueil (~0.15‰ offset) persists despite heating both groups of samples to ~116°C for 2 to 4 hours to remove adsorbed water, which indicates that any terrestrial contamination in the Orgueil samples is part of the structure of the minerals and not adsorbed to surfaces.

Dolomite grains in the Ryugu samples are enriched in ^{18}O, relative to the whole-rock values, but have $\Delta^{17}O$ values consistent with those of the whole rock (Fig. 4). The constituent minerals are generally consistent with mass-dependent fractionation. The oxygen isotope ratios of dolomite in Ryugu overlap with those of dolomite from Ivuna (Fig. 4). Ryugu magnetite is depleted in ^{18}O, relative to the whole-rock value, with all but one measurement being consistent with mass fractionation. The oxygen isotope ratios of Ryugu magnetite grains are consistent with those of Ivuna (*26*, *27*). The distributions of $^{18}O/^{16}O$ ratios and the consistency of $\Delta^{17}O$ values indicate isotopic equilibrium during the growth of the minerals that were produced during aqueous alteration.

In one polished section, dolomite and magnetite grains are located within ~100 μm of each other (fig. S1). The dolomite $\Delta^{17}O$ value is −0.7 ± 0.9‰ (2 SD) (*12*), whereas the magnetite grains have consistent $\Delta^{17}O$ values, with a mean of −0.1 ± 0.4‰ (2 SE). Because the $\Delta^{17}O$ values of dolomite and magnetite grains are within their mutual uncertainties, they might have precipitated from the same fluid. Assuming isotopic equilibrium, we used oxygen isotope thermometry (*28*–*31*) to estimate the temperature at which the dolomite-magnetite pair precipitated. The $\delta^{18}O$ values of the dolomite and magnetite are 29.9 ± 0.9‰ (2 SD) and −3.0 ± 1.1‰ (2 SD), respectively. The difference in $\delta^{18}O$ values between the dolomite and magnetite is 32.9 ± 1.4‰, which corresponds to an equilibration temperature of 37° ± 10°C (fig. S2). The temperature is in the range (10° to 150°C) of previous estimates for aqueous alteration of CI chondrites (*25*, *32*–*34*). We also estimated (*12*) the oxygen isotope ratios of the water and serpentine that would have been in

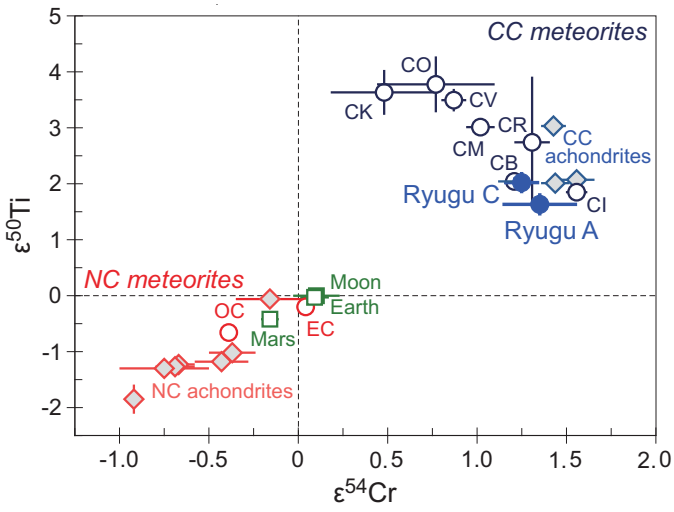

Fig. 3. Ti and Cr isotopes for Ryugu and other Solar System materials. Data are shown in epsilon notation, as defined by eqs. S1 and S2. The Ryugu samples (filled blue circles) are most similar to the CB and CI chondrites, in the CC meteorites region. Abbreviations are as follows: CC, carbonaceous (dark blue symbols); NC, noncarbonaceous (red symbols); CI, CM, CO, CV, CK, CR, and CB, named groups of carbonaceous chondrite meteorites; OC, ordinary chondrite meteorites; and EC, enstatite chondrite meteorites (all empty circles). The CC achondrites and NC achondrites (filled diamonds) are differentiated stony meteorites that have Ti and Cr isotopic compositions similar to those of CC and NC meteorites, respectively. Values for Earth, the Moon, and Mars are shown for comparison (empty green squares). Error bars are 2 SD of the mean. Data are from (*21*, *54*, *55*), except Ryugu (this work). Numeric values are provided in data S3.

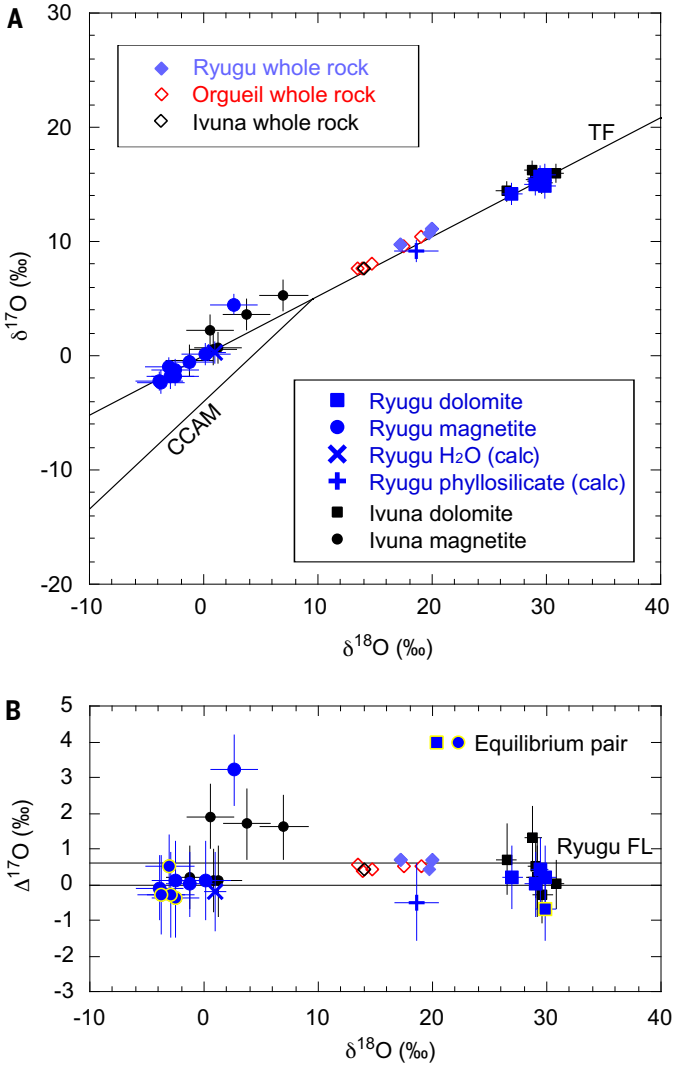

Fig. 4. Oxygen isotopes in Ryugu, Ivuna, and Orgueil. (**A**) $\delta^{17}O$ as a function of $\delta^{18}O$. Data are shown in δ notation, which is defined as the permille deviation from standard mean ocean water; see eq. S3. TF indicates the terrestrial mass fractionation line, which corresponds to mass-dependent isotope fractionations on Earth. CCAM indicates the carbonaceous chondrite anhydrous mineral line, which corresponds to the mass-independent isotope fractionations observed in refractory inclusions in chondrite meteorites. The Ryugu samples (solid blue symbols) are similar to the CI chondrites (black symbols for Ivuna and red for Orgueil). Oxygen isotopic compositions of H_2O (cross symbol) and phyllosilicates (plus symbol) in samples of Ryugu were calculated from values of dolomite and magnetite [blue symbols outlined in yellow in (B)] from the locations shown in fig. S1. (**B**) $\Delta^{17}O$ as a function of $\delta^{18}O$. The Δ notation is defined as the permille deviation from the TF line; see eq. S4. Ryugu FL indicates the mass-dependent fractionation line of Ryugu, which is derived by fitting a linear model to the Ryugu whole-rock data (*12*). In both (A) and (B), the error bars are 2 SD. Numeric values are provided in data S4.

equilibrium with those of the magnetite and dolomite grains and found ($\delta^{18}O$, $\delta^{17}O$) = (1.0 ± 1.0‰, 0.3 ± 1.0‰) for the water and (18.6 ± 2.0‰, 9.2 ± 1.0‰) for the serpentine (Fig. 4 and fig. S2). The value for serpentine is consistent with that of the whole rock, which is what we expected because of the high abundance of serpentine in the samples. These measurements indicate that oxygen isotopes were in equilibrium, or close to it, during aqueous alteration of the Ryugu samples.

^{53}Mn-^{53}Cr dating

The precipitation of dolomite and magnetite during aqueous alteration was dated using the ^{53}Mn-^{53}Cr system (*12*), which is based on the decay of the short-lived radionuclide ^{53}Mn to ^{53}Cr (half-life of 3.7 million years). The ^{53}Mn-^{53}Cr systems for dolomite in the Ryugu and Ivuna samples (Fig. 5) were measured from the polished section used for petrology and mineralogy using SIMS (*12*).

The slopes of linear models fitted to the data indicate initial ^{53}Mn/^{55}Mn ratios of $(2.55 \pm 0.35) \times 10^{-6}$ (2 SD) for Ryugu and $(3.14 \pm 0.28) \times 10^{-6}$ (2 SD) for Ivuna (*12*). Both initial values are consistent with those of CI dolomites that were obtained in previous studies (*35*, *36*). We compared the initial ^{53}Mn/^{55}Mn ratio to that of the D'Orbigny meteorite (*37*), an angrite that has been precisely dated and can be related to the ages of the oldest CAIs from CV (Vigarano-type) chondrites (*38*–*40*). We found that dolomite precipitation in the Ryugu sample occurred at $5.2^{+0.8}_{-0.7}$ million years after the oldest CAI formation, which is conventionally used to represent the formation of the Solar System. However, there is additional systematic uncertainty in this dolomite precipitation date because the initial Solar System ratio of ^{53}Mn/^{55}Mn is not precisely constrained. If we adopt different initial ^{53}Mn/^{55}Mn ratios than those found for D'Orbigny, the dolomite precipitation date changes to 4.8 million years [using the value in (*41*)] or 6.8 million years [for the value in (*42*)] after CAI formation. There may be additional systematic uncertainty in the ^{53}Mn-^{53}Cr age due to inherent analytical limitations of the measurement technique (*12*). We conclude that the Ryugu precipitation date is in the range of 3.1 million to 6.8 million years after CAI formation.

H_2O and CO_2 sources

Gas-release curves were measured for Ryugu samples from the first touchdown site (particle samples of A0040 and A0094) and Ivuna. Gas release was measured by increasing heating temperatures using thermogravimetric analysis coupled with mass spectrometry (TG-MS) and combination analyses of pyrolysis and combustion (EMIA-Step) (*12*). The mass decrease of the samples during heating (mass loss) was measured simultaneously.

The mass loss and differential mass loss [derivative thermogravimetric (DTG)] curves (*12*) for our Ryugu and Ivuna samples are shown in Fig. 6 [see also (*12*)]. The results for Ivuna are similar to those reported in previous studies (*43*). For Ryugu, we found a total mass loss of 15.38 ± 0.50 wt %, which is ~30% smaller than that of Ivuna (data S6). The species responsible for the mass loss are mainly H_2O and CO_2 for both Ivuna and Ryugu (Fig. 6). SO_2 might also contribute substantially, but we were unable to quantify it because of a lack of an appropriate standard (*12*).

The total weight fractions of H_2O and CO_2 gases released from the Ryugu sample that were measured using TG-MS are larger (20.78 ± 1.40 wt %) than the total mass loss (15.38 ± 0.50 wt %) that was measured using TG alone (*12*). We interpret this as indicating that carbonates were not the only sources of CO_2 during the TG-MS measurement, with organic carbon being oxidized to CO_2 by residual O_2 in the He gas flow used for the experiment, which produced a spurious excess of CO_2 in the mass spectrometry. Because decomposition of carbonates occurs within a small temperature range (*43*), we assigned the sharp CO_2 peaks at 600° to 800°C (Fig. 6) to carbonates. We observed two carbonate peaks for the Ryugu samples, which, according to the petrographic results above, contain three types of carbonate (dolomite, breunnerite, and calcite). We were unable to attribute specific peaks to specific carbonates. The double peaks might arise from sealed pore spaces because we analyzed intact chips and not powders.

The remaining broad continuum in Fig. 6 is probably due to the oxidation of organic carbon by the indigenous oxygen that is contained in organics in the sample or by residual O_2 in the He gas flow. Therefore, we assigned the CO_2 peak to carbonates and the remainder to organics (Fig. 6). The organic carbon content values are lower limits, because TG-MS leaves some organic carbon in the sample. The organic carbon and total carbon concentrations that we found using TG-MS were lower than those measured using EMIA-Step (*12*) (data S6). We estimate that 74 ± 3% of Ryugu organic carbon was released in TG-MS, as the broad organic carbon continuum, and 93 ± 4% for Ivuna. The profiles of the broad organic carbon continuum are different for both samples, which indicates differing organic components in Ryugu and Ivuna.

Many peaks are apparent in the H_2O release curves (Fig. 6). We identified adsorbed H_2O from sulfates released at ~250°C and a larger amount of H_2O from phyllosilicates

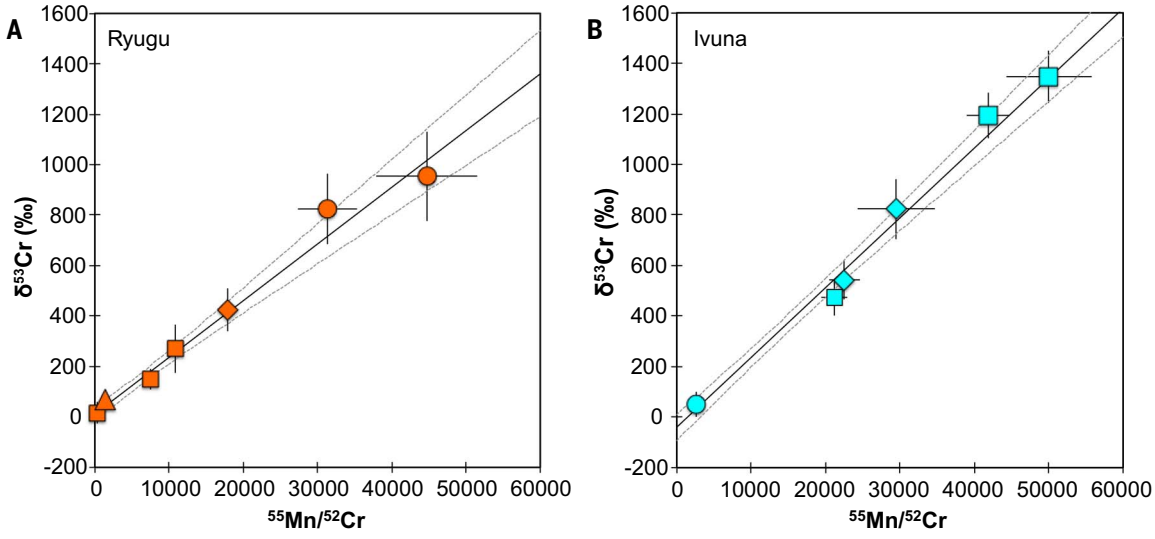

Fig. 5. ^{53}Mn-^{53}Cr isotopes measured from dolomite. (**A** and **B**) Data are shown for samples of (A) Ryugu and (B) Ivuna. Each symbol shape corresponds to measurements of a single crystal. The solid straight lines are least squares regression lines fitted to the data, and the dashed curves show 2σ confidence limits (*12*). The regression for Ryugu (*12*) indicates that dolomite precipitation occurred $5.2^{+0.8}_{-0.7}$ million years after the birth of the Solar System (there are additional systematic uncertainties on this value; see the text). Error bars are 2 SD. Numeric values are provided in data S5.

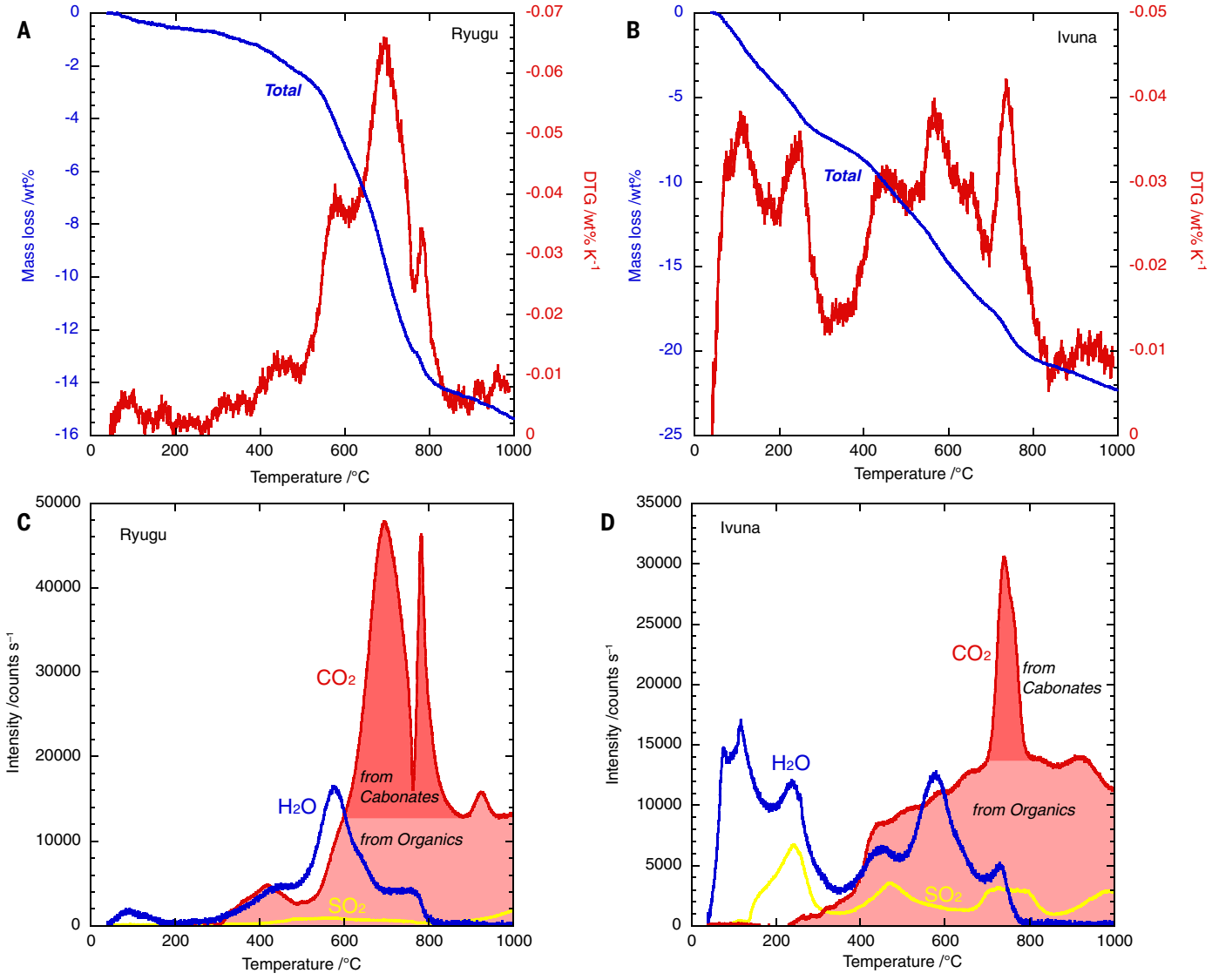

Fig. 6. TG-MS for Ryugu and Ivuna. (**A** to **D**) Mass loss (blue, left axis) and differential of mass-loss (DTG; red, right axis) curves are shown for (A) Ryugu and (B) Ivuna. Derived mass intensity curves are shown for (C) Ryugu and (D) Ivuna. The H_2O trace (blue) is for mass-to-charge ratio (m/z) = 18, CO_2 (red line) for m/z = 44, and SO_2 (yellow) for m/z = 64. Contributions of CO_2 are assigned to carbonates (red shading) and organics (pink shading). Numeric values are provided in data S7 (*12*).

at ~600°C. The phyllosilicates consist of serpentine and saponite (Fig. 1C). Serpentine contains structural OH sites in the crystal structure, whereas saponite contains interlayer H_2O in addition to structural OH sites. The petrologic and mineralogic observations suggest that the sulfate contribution is negligible for Ryugu but not for Ivuna. The SO_2 and H_2O peak releases coincide in Ivuna (at both 250° and 450°C) but not in Ryugu. We conclude that phyllosilicates are the dominant source of the H_2O that is released from the Ryugu sample.

Dehydration of the interlayer H_2O of saponite is complete at 170°C (peaking at 90°C) for Ryugu and complete at 350°C (peaking at 100°C) for Ivuna. Dehydroxylation of structural OH in saponite and serpentine occurs at 300° to 800°C for Ryugu and at 350° to 800°C for Ivuna. The structural OH is dominant (6.54 ± 0.32 wt % H_2O) in the Ryugu sample, with smaller amounts of interlayer H_2O (0.30 ± 0.01 wt % H_2O). Both forms of H_2O are present at similar levels in Ivuna (data S6).

Organic-inorganic fractions for hydrogen and carbon

We performed an EMIA-Step analysis of the Ryugu and Ivuna samples (*12*). For Ivuna, the results showed that the total carbon concentration is 3.31 ± 0.33 wt % (*12*), of which 90% is organic carbon (Fig. 7 and data S6). The total hydrogen in Ivuna is 1.59 ± 0.08 wt %, of which 89% is inorganic hydrogen. All these values are consistent with previous measurements of the same meteorite (*44*). The total H_2O for Ivuna is 12.73 ± 0.63 wt %, distributed as 6.58 ± 0.32 wt % interlayer H_2O and 6.15 ± 0.30 wt % structural OH or H_2O in the phyllosilicate minerals.

The Ryugu samples contain less H_2O than Ivuna. The total H_2O is 6.84 ± 0.34 wt %, including 0.30 ± 0.01 wt % interlayer H_2O and 6.54 ± 0.32 wt % structural OH or H_2O (data S6). The structural value is similar to that of Ivuna, but the interlayer water value is substantially lower. The total hydrogen is 0.94 ± 0.05 wt % for Ryugu, and the inorganic hydrogen (i.e., H_2O) makes up 81% of the total hydrogen. The amount of organic

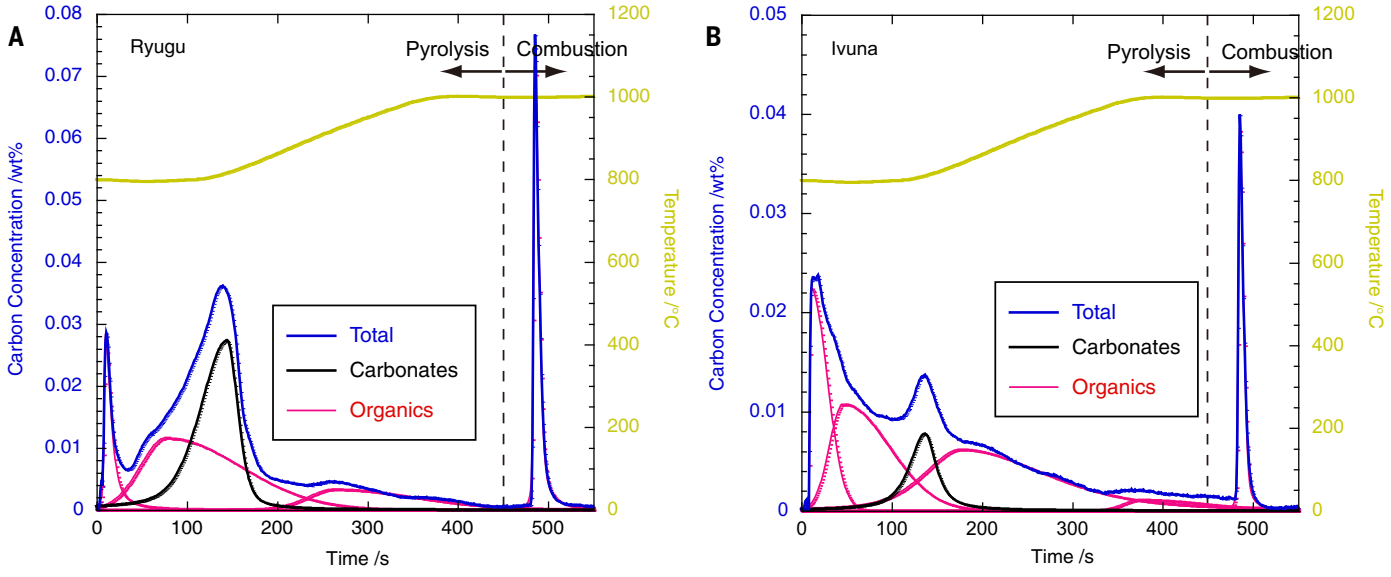

Fig. 7. Combination analyses of pyrolysis and combustion (EMIA-Step) for Ryugu and Ivuna. (**A** and **B**) Carbon release curves are shown for (A) Ryugu and (B) Ivuna. The carbon concentration (blue, left axis) is plotted as a function of the sample heating time (*x* axis). The sample temperature (yellow, right axis) changes nonlinearly with time. The dashed line at 450 s shows the boundary between conditions of pyrolysis and combustion (*12*). The integration under each blue curve corresponds to the total carbon released from the sample. These contributions are deconvolved and assigned to different carbonates (black) and organics (pink) in the sample (*12*); the integration under these curves corresponds to inorganic and organic carbon concentrations, respectively. Numeric values are provided in data S8.

carbon in Ryugu is 3.08 ± 0.30 wt %, which is indistinguishable from that in Ivuna (2.97 ± 0.29 wt %) (Fig. 7 and data S6). This implies that the inorganic matter/organic matter ratio is similar in the Ryugu and Ivuna samples that were studied, excluding a previous proposal that Ryugu's low albedo is due to Ryugu having higher organic carbon contents than CI chondrites (*45*). However, the total carbon is higher in Ryugu (4.63 ± 0.23 wt %) than in Ivuna, owing to the higher abundances of carbonates in the Ryugu samples.

Formation history of Ryugu

Ryugu is thought to have formed through the reaccumulation of material ejected from a parent body by an impact (*5*). The aqueous alteration of the samples must have occurred on the parent body because aqueous fluid is not stable in the current Ryugu asteroid. The CI-like elemental abundances of Ryugu suggest that the parent body accreted all elements with 50% condensation temperatures higher than 500 K that were present at the formation of the Solar System, along with some ice-forming elements (Fig. 2). Ryugu's parent body was probably closely related to the parent body (or bodies) of the CI chondrites. We assume that the accreted material was mainly anhydrous dust and ice. Physical modeling of the thermal evolution of a water ice–bearing CI-like planetesimal (*35*), compared with the results of our oxygen-isotope thermometry, suggests that the Ryugu parent body accreted 2 million to 4 million years after the formation of the Solar System (as defined by the ages of the oldest CAIs).

About 1 million to 2 million years later, roughly 5 million years after the formation of the Solar System (Fig. 5), the material that would later be incorporated into Ryugu experienced aqueous alteration. This caused the precipitation of dolomite and magnetite from an aqueous solution at about 37°C. The aqueous alteration of the primary minerals was very extensive. The saponite produced by this fluid-assisted alteration in the parent body must have contained large amounts of interlayer water (~7 wt %) in its crystal structure when it formed under saturated water activity, as observed in Ivuna (data S6). The low abundance of interlayer water in the Ryugu samples (0.3 wt %) indicates that much of this water later escaped to space, most likely after disruption of the parent body and formation of the rubble-pile asteroid Ryugu. We cannot definitively identify the dehydration mechanism but suggest that it may have included some combination of impact heating, solar heating, space weathering, and long-term exposure of the asteroid surface to the ultrahigh vacuum of space.

We estimate the dehydration temperature as 170°C, the temperature at which interlayer water that is now in the Ryugu samples completely dehydrates. The dehydration speed of the interlayer water in our experiments is 20% of the total interlayer water per minute, around the peak temperature of 90°C (data S7) (*12*). The ambient space pressure in Ryugu, which is much lower than the experimental pressure of 10^5 Pa, would accelerate this dehydration speed. Such high dehydration rates are sufficient to completely dehydrate the interlayer water for any plausible geological heating events that occurred in Ryugu. Because a small peak of interlayer water is still emitted at 90°C in our experiments, it is possible that, since their aqueous alteration, the Ryugu samples have never been heated above ~100°C (Fig. 6). These temperatures rule out the previously proposed thermal history of Ryugu (*6*), which was based on laboratory heating experiments of carbonaceous chondrites. The temperatures that we estimate are consist with Hayabusa2 observations of the surface temperature at the present orbit of Ryugu (*7*).

Some asteroids show comet-like activity, the origin of which is uncertain and could involve several mechanisms (*46*). This activity can be subtle, as in the B-type (bluish and spectroscopically similar to C-type) asteroid Bennu, where small ejections of dust particles and rocks have been observed (*47*). Thermal fracturing, phyllosilicate dehydration, and micrometeoroid impacts have been proposed (*47*) as explanations for the ejection of solid particles from Bennu. Our finding that saponite in Ryugu is partially dehydrated supports the possibility that volatile release from phyllosilicates can induce comet-like activity at the surface of inner Solar System

carbonaceous asteroids. Possible mechanisms to lift dust and rocks from asteroid surfaces include (i) anisotropic release of water molecules from phyllosilicate-rich dust particles, which imparts a net momentum to those particles, or (ii) buildup of vapor pressure in sealed pore spaces, which leads to pore bursting that propels dust particles away from the surface. Phyllosilicate dehydration could also play a role in the production of interplanetary dust particles and micrometeorites. The thermal release pattern of Ivuna (Fig. 6) shows that interlayer water is lost from saponite at a temperature between ~0° and 200°C. The observed maximum current surface temperatures of ~100°C for Ryugu (*7*) and ~170°C for Bennu (*48*) would therefore be sufficient for such devolatilization to take place. If so, the devolatilization must be largely complete for surface particles on Ryugu because no particle ejections were observed by the Hayabusa2 spacecraft.

Implications for CI chondrites and cosmochemistry

The elemental compositions of CI chondrites more closely match measurements of the solar photosphere than those of other types of meteorites (*49*); CIs differ from the Sun in the abundances of the noble gases, hydrogen, carbon, nitrogen, oxygen, and lithium. CI chondrites experienced pervasive aqueous alteration during water-rock interactions in the early Solar System. Fewer than a dozen CI chondrites are known, and they have all been on Earth for decades to centuries (the most recent fall was in 1965). It is therefore unknown how much handling and exposure to atmospheric moisture has modified their mineralogies and elemental compositions. Unlike CI chondrites, the Ryugu samples are nearly free of sulfates, ferrihydrite, and interlayer water. This could be due to CI chondrites either having originated on parent asteroids with higher water contents than Ryugu or having been contaminated by terrestrial moisture during their residence on Earth (*50*, *51*). The lower abundance of anhydrous silicates, and the small but measurable offset in $\Delta^{17}O$ between Ryugu and the Orgueil CI chondrite (Fig. 4), supports the terrestrial contamination explanation. The slightly higher $\Delta^{17}O$ values of Orgueil in this study compared with those in earlier studies could be explained if O-isotope exchange in the structural OH water of CI chondrites occurred under room-temperature conditions. The gas emission patterns measured in the TG-MS and EMIA-Step analyses of Ryugu differ from those of the Ivuna CI chondrite (Figs. 6 and 7). This suggests that the structures of the organic matter differ between Ryugu samples and Ivuna, possibly because of modification during their residence on Earth.

We conclude that the Ryugu samples are more chemically pristine than other Solar System materials that have been analyzed in laboratories, including CI meteorites. The materials observed in CI chondrites may have been modified on Earth and thus no longer reflect their states in space. Possible causes are phyllosilicate hydration, organic matter transformation and contamination, adsorption or reaction of atmospheric components, and oxidation. These modifications might have changed the albedo, porosity, and density of the CI chondrites, which could explain the differences between CIs and the observations of Ryugu by Hayabusa2 (*5*, *7*) and between CIs and the Ryugu samples returned to Earth (*10*).

REFERENCES AND NOTES

1. H. Yurimoto *et al*., Oxygen isotopic compositions of asteroidal materials returned from Itokawa by the Hayabusa mission. *Science* **333**, 1116–1119 (2011). doi: 10.1126/science.1207776; pmid: 21868668
2. T. Nakamura *et al*., Itokawa dust particles: A direct link between S-type asteroids and ordinary chondrites. *Science* **333**, 1113–1116 (2011). doi: 10.1126/science.1207758; pmid: 21868667
3. S. Tachibana *et al*., Hayabusa2: Scientific importance of samples returned from C-type near-Earth asteroid (162173) 1999 JU_3. *Geochem. J.* **48**, 571–587 (2014). doi: 10.2343/geochemj.2.0350
4. K. Kitazato *et al*., The surface composition of asteroid 162173 Ryugu from Hayabusa2 near-infrared spectroscopy. *Science* **364**, 272–275 (2019). doi: 10.1126/science.aav7432; pmid: 30890589
5. S. Sugita *et al*., The geomorphology, color, and thermal properties of Ryugu: Implications for parent-body processes. *Science* **364**, 252 (2019). doi: 10.1126/science.aaw0422; pmid: 30890587
6. K. Kitazato *et al*., Thermally altered subsurface material of asteroid (162173) Ryugu. *Nat. Astron.* **5**, 246–250 (2021). doi: 10.1038/s41550-020-01271-2
7. T. Okada *et al*., Highly porous nature of a primitive asteroid revealed by thermal imaging. *Nature* **579**, 518–522 (2020). doi: 10.1038/s41586-020-2102-6; pmid: 32214245
8. M. Grott *et al*., Low thermal conductivity boulder with high porosity identified on C-type asteroid (162173) Ryugu. *Nat. Astron.* **3**, 971–976 (2019). doi: 10.1038/s41550-019-0832-x
9. T. Morota *et al*., Sample collection from asteroid (162173) Ryugu by Hayabusa2: Implications for surface evolution. *Science* **368**, 654–659 (2020). doi: 10.1126/science.aaz6306; pmid: 32381723
10. T. Yada *et al*., Preliminary analysis of the Hayabusa2 samples returned from C-type asteroid Ryugu. *Nat. Astron.* **6**, 214–220 (2021). doi: 10.1038/s41550-021-01550-6
11. S. Tachibana *et al*., Pebbles and sand on asteroid (162173) Ryugu: In situ observation and particles returned to Earth. *Science* **375**, 1011–1016 (2022). doi: 10.1126/science.abj8624; pmid: 35143255
12. See supplementary materials.
13. A. J. Brearley, in *Meteorites and the Early Solar System II*, D. S. Lauretta, H. Y. McSween, Eds. (Univ. of Arizona Press, 2006), pp. 587–624.
14. N. Dauphas, A. Pourmand, Thulium anomalies and rare earth element patterns in meteorites and Earth: Nebular fractionation and the nugget effect. *Geochim. Cosmochim. Acta* **163**, 234–261 (2015). doi: 10.1016/j.gca.2015.03.037
15. A.-C. Zhang *et al*., Young asteroidal fluid activity revealed by absolute age from apatite in carbonaceous chondrite. *Nat. Commun.* **7**, 12844 (2016). doi: 10.1038/ncomms12844; pmid: 27682449
16. A. Morlok *et al*., Brecciation and chemical heterogeneities of CI chondrites. *Geochim. Cosmochim. Acta* **70**, 5371–5394 (2006). doi: 10.1016/j.gca.2006.08.007
17. J. A. Barrat *et al*., Geochemistry of CI chondrites: Major and trace elements, and Cu and Zn isotopes. *Geochim. Cosmochim. Acta* **83**, 79–92 (2012). doi: 10.1016/j.gca.2011.12.011
18. C. M. O'D. Alexander, R. Bowden, M. L. Fogel, K. T. Howard, Carbonate abundances and isotopic compositions in chondrites. *Meteorit. Planet. Sci.* **50**, 810–833 (2015). doi: 10.1111/maps.12410
19. J. T. Wasson, G. W. Kallemeyn, Compositions of chondrites. *Philos. Trans. R. Soc. Lond. A* **325**, 535–544 (1988). doi: 10.1098/rsta.1988.0066
20. P. H. Warren, Stable-isotopic anomalies and the accretionary assemblage of the Earth and Mars: A subordinate role for carbonaceous chondrites. *Earth Planet. Sci. Lett.* **311**, 93–100 (2011). doi: 10.1016/j.epsl.2011.08.047
21. A. Trinquier *et al*., Origin of nucleosynthetic isotope heterogeneity in the solar protoplanetary disk. *Science* **324**, 374–376 (2009). doi: 10.1126/science.1168221; pmid: 19372428
22. T. Kleine *et al*., The non-carbonaceous–carbonaceous meteorite dichotomy. *Space Sci. Rev.* **216**, 55 (2020). doi: 10.1007/s11214-020-00675-w
23. I. Leya, M. Schönbächler, U. Wiechert, U. Krähenbühl, A. N. Halliday, Titanium isotopes and the radial heterogeneity of the solar system. *Earth Planet. Sci. Lett.* **266**, 233–244 (2008). doi: 10.1016/j.epsl.2007.10.017
24. A. N. Krot, K. Keil, E. R. D. Scott, C. A. Goodrich, M. K. Weisberg, in *Treatise on Geochemistry*, H. D. Holland, K. K. Turekian, Eds. (Elsevier, ed. 2, 2014), pp. 1–63.
25. R. N. Clayton, T. K. Mayeda, Oxygen isotope studies of carbonaceous chondrites. *Geochim. Cosmochim. Acta* **63**, 2089–2104 (1999). doi: 10.1016/S0016-7037(99)00090-3
26. M. W. Rowe, R. N. Clayton, T. K. Mayeda, Oxygen isotopes in separated components of CI and CM meteorites. *Geochim. Cosmochim. Acta* **58**, 5341–5347 (1994). doi: 10.1016/0016-7037(94)90317-4
27. M. Piralla *et al*., Primordial water and dust of the Solar System: Insights from in situ oxygen measurements of CI chondrites. *Geochim. Cosmochim. Acta* **269**, 451–464 (2020). doi: 10.1016/j.gca.2019.10.041
28. Y. Zheng, Calculation of oxygen isotope fractionation in metal oxides. *Geochim. Cosmochim. Acta* **55**, 2299–2307 (1991). doi: 10.1016/0016-7037(91)90105-E
29. Y.-F. Zheng, Oxygen isotope fractionation in carbonate and sulfate minerals. *Geochem. J.* **33**, 109–126 (1999). doi: 10.2343/geochemj.33.109
30. Y.-F. Zheng, On the theoretical calculations of oxygen isotope fractionation factors for carbonate-water systems. *Geochem. J.* **45**, 341–354 (2011). doi: 10.2343/geochemj.1.0125
31. Y.-F. Zheng, Calculation of oxygen isotope fractionation in hydroxyl-bearing silicates. *Earth Planet. Sci. Lett.* **120**, 247–263 (1993). doi: 10.1016/0012-821X(93)90243-3
32. W. Guo, thesis, California Institute of Technology (2009).
33. R. Visser, T. John, M. Menneken, M. Patzek, A. Bischoff, Temperature constraints by Raman spectroscopy of organic matter in volatile-rich clasts and carbonaceous chondrites. *Geochim. Cosmochim. Acta* **241**, 38–55 (2018). doi: 10.1016/j.gca.2018.08.037
34. M. E. Zolensky, W. L. Bourcier, J. L. Gooding, Aqueous alteration on the hydrous asteroids: Results of EQ3/6 computer simulations. *Icarus* **78**, 411–425 (1989). doi: 10.1016/0019-1035(89)90188-7
35. W. Fujiya, N. Sugiura, Y. Sano, H. Hiyagon, Mn-Cr ages of dolomites in CI chondrites and the Tagish Lake ungrouped carbonaceous chondrite. *Earth Planet. Sci. Lett.* **362**, 130–142 (2013). doi: 10.1016/j.epsl.2012.11.057
36. R. Visser, T. John, M. J. Whitehouse, M. Patzek, A. Bischoff, A short-lived ^{26}Al induced hydrothermal alteration event in the outer solar system: Constraints from Mn/Cr ages of carbonates. *Earth Planet. Sci. Lett.* **547**, 116440 (2020). doi: 10.1016/j.epsl.2020.116440
37. D. P. Glavin, A. Kubny, E. Jagoutz, G. W. Lugmair, Mn-Cr isotope systematics of the D'Orbigny angrite. *Meteorit. Planet. Sci.* **39**, 693–700 (2004). doi: 10.1111/j.1945-5100.2004.tb00112.x
38. G. A. Brennecka, M. Wadhwa, Uranium isotope compositions of the basaltic angrite meteorites and the chronological implications for the early Solar System. *Proc. Natl. Acad. Sci. U.S.A.* **109**, 9299–9303 (2012). doi: 10.1073/pnas.1114043109; pmid: 22647606
39. J. N. Connelly *et al*., The absolute chronology and thermal processing of solids in the solar protoplanetary disk. *Science* **338**, 651–655 (2012). doi: 10.1126/science.1226919; pmid: 23118187
40. F. L. H. Tissot, N. Dauphas, T. L. Grove, Distinct $^{238}U/^{235}U$ ratios and REE patterns in plutonic and volcanic angrites: Geochronologic implications and evidence for U isotope fractionation during magmatic processes. *Geochim. Cosmochim. Acta* **213**, 593–617 (2017). doi: 10.1016/j.gca.2017.06.045

41. A. Trinquier, J. L. Birck, C. J. Allègre, C. Göpel, D. Ulfbeck, ^{53}Mn–^{53}Cr systematics of the early Solar System revisited. *Geochim. Cosmochim. Acta* **72**, 5146–5163 (2008). doi: 10.1016/j.gca.2008.03.023
42. L. E. Nyquist, T. Kleine, C. Y. Shih, Y. D. Reese, The distribution of short-lived radioisotopes in the early solar system and the chronology of asteroid accretion, differentiation, and secondary mineralization. *Geochim. Cosmochim. Acta* **73**, 5115–5136 (2009). doi: 10.1016/j.gca.2008.12.031
43. A. J. King, J. R. Solomon, P. F. Schofield, S. S. Russell, Characterising the CI and CI-like carbonaceous chondrites using thermogravimetric analysis and infrared spectroscopy. *Earth Planets Space* **67**, 198 (2015). doi: 10.1186/s40623-015-0370-4
44. C. M. O'D. Alexander *et al*., The provenances of asteroids, and their contributions to the volatile inventories of the terrestrial planets. *Science* **337**, 721–723 (2012). doi: 10.1126/science.1223474; pmid: 22798405
45. C. Potiszil, R. Tanaka, K. Kobayashi, T. Kunihiro, E. Nakamura, The albedo of Ryugu: Evidence for a high organic abundance, as inferred from the Hayabusa2 touchdown maneuver. *Astrobiology* **20**, 916–921 (2020). doi: 10.1089/ast.2019.2198; pmid: 32543220
46. D. Jewitt, H. Hsieh, J. Agarwal, in *Asteroids IV*, P. Michel, F. E. DeMeo, W. F. Bottke, Eds. (Univ. of Arizona Press, 2015), pp. 221–241.
47. D. S. Lauretta *et al*., Episodes of particle ejection from the surface of the active asteroid (101955) Bennu. *Science* **366**, eaay3544 (2019). doi: 10.1126/science.aay3544; pmid: 31806784
48. D. N. DellaGiustina *et al*., Properties of rubble-pile asteroid (101955) Bennu from OSIRIS-REx imaging and thermal analysis. *Nat. Astron.* **3**, 341–351 (2019). doi: 10.1038/s41550-019-0731-1
49. K. Lodders, Relative atomic solar system abundances, mass fractions, and atomic masses of the elements and their isotopes, composition of the solar photosphere, and compositions of the major chondritic meteorite groups. *Space Sci. Rev.* **217**, 44 (2021). doi: 10.1007/s11214-021-00825-8
50. M. Gounelle, M. E. Zolensky, The Orgueil meteorite: 150 years of history. *Meteorit. Planet. Sci.* **49**, 1769–1794 (2014). doi: 10.1111/maps.12351
51. L. Baker, I. A. Franchi, I. P. Wright, C. T. Pillinger, The oxygen isotopic composition of water from Tagish Lake: Its relationship to low-temperature phases and to other carbonaceous chondrites. *Meteorit. Planet. Sci.* **37**, 977–985 (2002). doi: 10.1111/j.1945-5100.2002.tb00870.x
52. A. Bischoff *et al*., The old, unique C1 chondrite Flensburg – Insight into the first processes of aqueous alteration, brecciation, and the diversity of water-bearing parent bodies and lithologies. *Geochim. Cosmochim. Acta* **293**, 142–186 (2021). doi: 10.1016/j.gca.2020.10.014
53. J. Alfing, M. Patzek, A. Bischoff, Modal abundances of coarse-grained (>5 μm) components within CI-chondrites and their individual clasts – Mixing of various lithologies on the CI parent body(ies). *Chem. Erde* **79**, 125532 (2019). doi: 10.1016/j.chemer.2019.08.004
54. N. Dauphas, E. A. Schauble, Mass Fractionation Laws, Mass-Independent Effects, and Isotopic Anomalies. *Annu. Rev. Earth Planet. Sci.* **44**, 709–783 (2016). doi: 10.1146/annurev-earth-060115-012157
55. C. Burkhardt *et al*., In search of the Earth-forming reservoir: Mineralogical, chemical, and isotopic characterizations of the ungrouped achondrite NWA 5363/NWA 5400 and selected chondrites. *Meteorit. Planet. Sci.* **52**, 807–826 (2017). doi: 10.1111/maps.12834

ACKNOWLEDGMENTS

We thank D. Rogers, M. Spicuzza, and J. Valley for their help with the carbonate standards for the SIMS analyses. We thank SPring-8 for allowing us to use their facilities. Hayabusa2 was developed and built under the leadership of the Japan Aerospace Exploration Agency (JAXA), with contributions from the German Aerospace Center (DLR) and the Centre National d'Études Spatiales (CNES) and in collaboration with NASA and other universities, institutes, and companies in Japan. The curation system was developed by JAXA in collaboration with companies in Japan. **Funding:** H.Yu., T.Yo., I.N., T.U., T.No., S.W., and S.Tac. acknowledge funding from Japan Society for the Promotion of Science (JSPS) KAKENHI grants. E.D.Y., L.N., and A.Ng. acknowledge funding from NASA grants. T.R.I. acknowledges an Australian Research Council grant. **Author contributions:** H.Yu. coordinated coauthor contributions and wrote the paper, with contributions from members of the Hayabusa2-initial-analysis chemistry team. H.Yu. led the TG-MS and EMIA-Step analyses, with contributions from Ho.H., S.Ko., and S.Tac. T.Yo. led the ICP-MS and TIMS analysis. K.N. led the SIMS analysis. I.N. led the XRF analysis. E.D.Y. led the LF-IRMS analysis. Y.Ab., J.A., C.M.O.A., S.A., Y.Am., K.B., M.B., A.B., R.W.C., M.C., B.-G.C., N.D., A.M.D., T.D.R., W.F., R.F., I.G., M.H., Y.Hib., H.Hi., H.Ho., P.H., G.R.H., K.I., T.Ii., T.R.I., A.I., M.It., S.I., N.K., N.T.K., K.Kitaj., T.K., S.Ko., A.N.K., M.-C.L., Y.Ma., K.D.M., M.Mo., K.Mo., F.M., A.Ng., L.N., M. On., A.P., C.P., L.P., L.Q., S.S.R., N.Sakam., M.S., L.T., H.Tan., K.T., Y.Te., T.U., S.Wad., M.W., R.J.W., K.Ya., Q.-Z.Y., S.Y., H.Yu., A.-C.Z., and S.Tac. assisted with the analyses. All authors discussed the results and commented on the manuscript. **Competing interests:** We declare no competing interests. **Data and materials availability:** Measurement values from each of our experiments are tabulated in data S1 to S9. All images and data tables used in this study are also available at the JAXA Data Archives and Transmission System (DARTS) at https://data.darts.isas.jaxa.jp/pub/hayabusa2/paper/sample/Yokoyama_2022/. Further data on the Hayabusa2 samples are available at the DARTS archive www.darts.isas.jaxa.jp/curation/hayabusa2. The samples of Ryugu are curated by the JAXA Astromaterials Science Research Group; distribution for analysis is through announcements of opportunity available at https://jaxa-ryugu-sample-ao.net. Details of the Orgueil and Ivuna samples that we used for comparison are provided in the supplementary materials.

SUPPLEMENTARY MATERIALS

Submitted 20 December 2021; accepted 25 May 2022
10.1126/science.abn7850